Modelling a reversible coupled wireless energy transfer system

1st Edouard Bonnar
4th year Student
Department of Computer and Electrical Engineering
INSA-Toulouse
Toulouse, France
bonnar-gaudr@insa-toulouse.fr

2nd Flavien Carvalho
4th year Student
Department of Computer and Electrical Engineering
INSA-Toulouse
Toulouse, France
fcarvalho@insa-toulouse.fr

3rd Julie Champagne
4th year Student
Department of Computer and Electrical Engineering
INSA-Toulouse
Toulouse, France
champagne@insa-toulouse.fr

4th Denis Lespiaucq
4th year Student
Department of Computer and Electrical Engineering
INSA-Toulouse
Toulouse, France
lespiaucq@insa-toulouse.fr

5th Raphaël Marques
4th year Student
Department of Computer and Electrical Engineering
INSA-Toulouse
Toulouse, France
rmarques@insa-toulouse.fr

6th Caroline Nguyen
4th year Student
Department of Computer and Electrical Engineering
INSA-Toulouse
Toulouse, France
c_nguyen@insa-toulouse.fr

7th Paul Pralus
4th year Student
Department of Computer and Electrical Engineering
INSA-Toulouse
Toulouse, France
pralus@insa-toulouse.fr

***Abstract*—Wireless power transfer, based on electromagnetic induction, is essential for short-range applications, particularly for mobile devices like electric vehicles and medical implants. However, coil misalignment can reduce transfer efficiency, requiring real-time measurement and optimization through a control algorithm. Additionally, for bidirectional systems such as vehicle-to-grid applications, the charger must support both battery charging and discharging. This research has two main objectives: to identify the parameters that will maximise the energy efficiency of the transfer, and then to calculate them and decide how to optimise the performance of wireless energy transfer in real time. It is built on previous work aimed at reducing the cost and weight of ferromagnetic materials while validating reversible power transfer. The methodology includes circuit modelling and simulation, followed by laboratory testing. It involves deriving a state-space model based on a simplified representation of the system using the first Fourier harmonic. The results enable real-time optimization of transfer efficiency using techniques such as mutual inductance measurement through the harmonics of the signal of the secondary coil applied to the primary coil with a radio communication link. The findings of this study had significant implications for improving contactless energy transfer systems, with potential applications in multiple fields. The next step will be to refine the models and conduct further tests to validate the proposed solutions.**

I. Introduction

The ongoing energy transition, driven by the increasing electrification of transportation and the rapid development of electric vehicles, presents new challenges in energy conversion. In particular, the growing demands for efficiency, safety, and bidirectional energy exchange in wireless charging systems have motivated the study andb optimization of high-performance converter topologies.

In this context, the Dual Active Bridge (DAB) has emerged as a preferred architecture for high-power applications, such as fast charging of electric vehicles. Introduced in the 1990s, the DAB offers decisive advantages, including galvanic isolation via a high-frequency transformer, inherent capability for bidirectional energy transfer, and high efficiency operation through phase-shift modulation techniques. This topology also stands out for its robustness against geometric misalignments of coils

in wireless power transfer systems, making it an ideal candidate for automated and intelligent charging infrastructures.

Among the variety of existing DC/DC converters (Buck, Boost, Flyback, Resonant, etc.), the DAB is distinguished not only by its typical efficiency of over 95%, but also by its control flexibility and compatibility with high-power charge/discharge requirements (up to several hundred kilowatts). Its ability to maintain optimal energy transfer even in cases of coil misalignment or load variations further enhances the appeal of this topology for advanced onboard or stationary systems. However, most research only applies to static misalignment and thus the parameters important for the optimization of the efficiency may vary over time.

This article aims to explore in detail key elements to maximize efficiency of the DAB converter in imperfect conditions like coil misalignment through control of its bridges by a Pulse Width Modulation (PWM).

II. Related work

Related Work DAB to condense in 1 page. If everything doesn't fit we can do "Magouille & compagnie" to put in elsewhere in the article

Related works - topology variants and technological choice?

III. Methods

A. Electrical command

As a way to control the DAB, it is possible to act on four parameters (including two parameters deduced from two others).

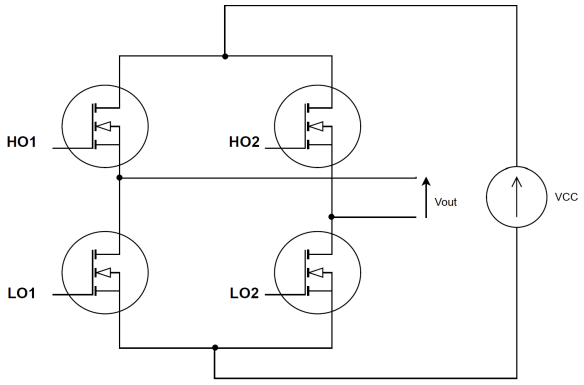

Fig. 1. H-Bridge electrical assembly

The duty cycle α that must be included in the interval $[0\%; 50\%[$ corresponds to the percentage of the period where the pair of MOSFET transistors (on primary side) [Q1, Q4] are conducting and in addition, the pair [Q2, Q3] are off.

The duty cycle β that also must be included in the interval $[0\%; 50\%[$ and corresponds to the percentage of the period where the pair of MOSFET transistors (on secondary side) [Q5, Q8] are conducting and in addition, the pair [Q6, Q7] are off. On each side, the duty cycle must always stay under 50% to avoid short-circuiting the supply voltage with the ground. If the duty cycle exceeds 50%, the two pairs of transistors will at some point start to conduct simultaneously and therefore will damage the power supply

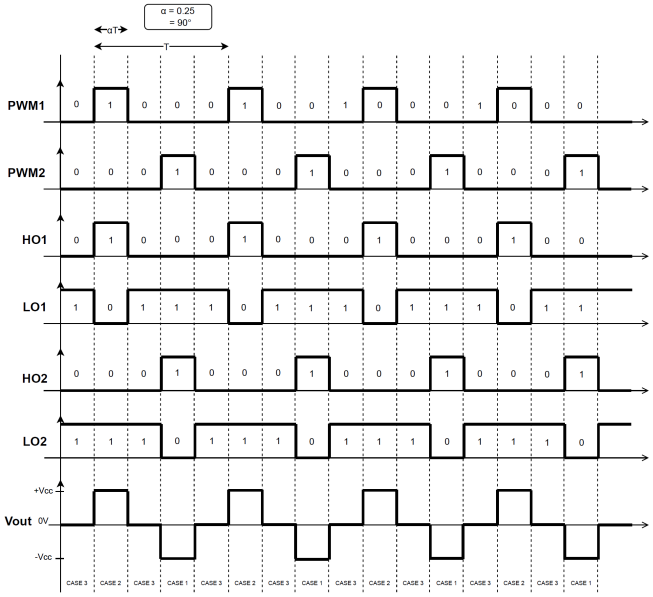

Fig. 2. 25% duty cycle control chronogram example

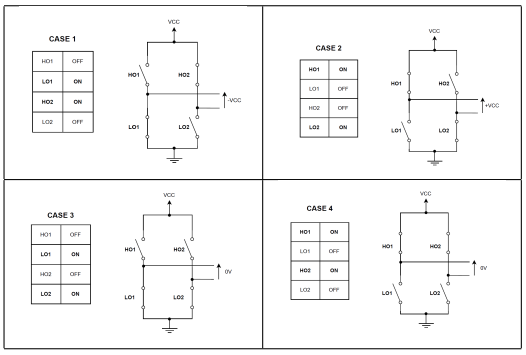

Fig. 3. All differents scenarios of control

The two others parameters linked and deduce from the two duty cycle are φ_P and, φ_S corresponding to the phase-shift between the two legs of the converter through $\alpha = 180° - \varphi_P$ and $\beta = 180° - \varphi_S$. Since the bridge consists of two H-bridges on one side at primary and then secondary level, there are similar dimensions on each side of the converter. We can express α or β in an angle unit or with a percentage. The duty cycle is between 0 and 100%, if we consider a period T , the time during the high state can be expressed as αT which can be called τ. So $\tau = \alpha T$. In fact, we can express T or τ with a time unit (s) or with an angle unit $(°)$. This leads to expressing α in degrees, considering a period as $360°$ or linearly. Such as $\alpha\,[°] = \alpha\,[linear] \times 360$.

B. Equations

We based our research on the bidirectional Wireless Power Transfer System with a series-series compensation from [1]. During the first part of our research, the circuit and the equation associated with was analysed to have a better understanding of the circuit and to ensure that there is no error in the paper. For the analysis, a diagram was made to see how the H bridge works to understand how it can be link to the simplified model of the article [1]. From the Vout chronogram, it can be deduced that the bridge behaviour can be assimilated to a sinusoidal signal by simplifying the bridge command with a first order approximation. From that analysis, the simplified model was used to find a State Space Model of this circuit by considering the transistor command as a sinusoid depending on the phase between the transistors. The aim here is to find a usable state space model to be able to control it with a command law. From the simplified model, the chosen states are i_p, u_cp, i_s, u_{cs}. To ensure that the model is usable and reliable, we have to verify the model via MATLAB and Simulink simulation and compare the circuit simulation to our model.

C. Python simulation

In order to graphically visualize the relationship between all the mathematical relations presented so far, a Python script was programmed. By adding a solver system linking the functions (X), (X) and (X), and with the MatPlotLib graphics library, the plot of power output as a function of variations in M and BETA was generated. The graphical figure resulting from the Python simulation is shown below: It may be worth pointing

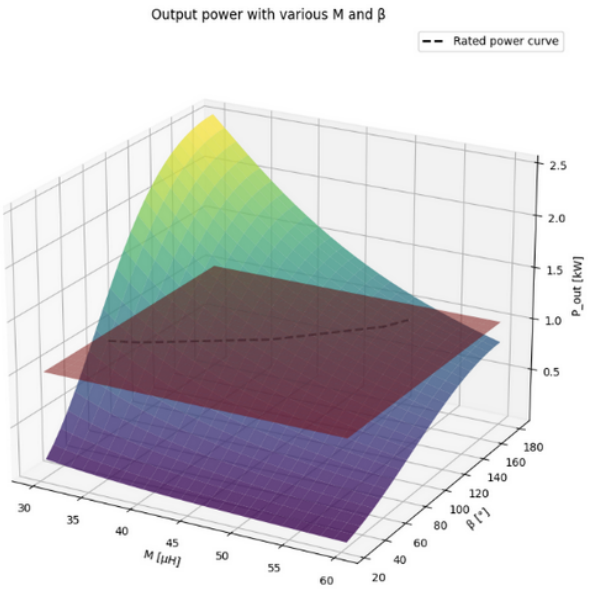

Fig. 4. Output power with various M and β

out that the article [X] contains some internal errors, notably on the annotation of their simulation allowing the graphical representation of power output with respect to the parameters M and β. Indeed, for a given output power of 1 kW and a mutual inductance M of 35 uH, the β angle obtained is 80.39° and not 83° as specified in the article.

D. Python simulation

1) LTSpice: An LTSpice simulation was made to model the expected behaviour of the system reliably, so that we could validate it and begin calculations to obtain its state space. So, by selecting MOSFET power transistors commonly used in Dual Active Bridge devices, with good efficiency to limit switching losses, and adding all the PWM control signals (PWM 1 to 8), it is possible to obtain a complete simulation of the system. In our case, the transistors are considered ideal, and the control output obtained corresponds to the expectations in ideal condition. The result can be seen in the chronogram below : However, in order to get closer result

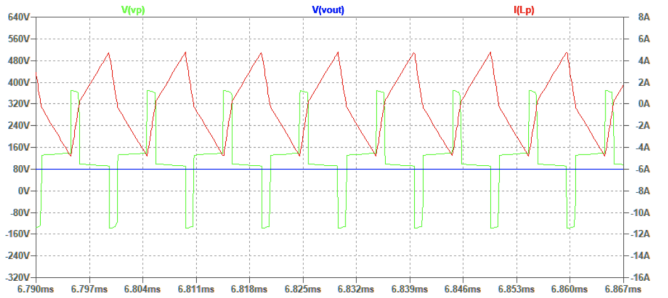

Fig. 5. Chronogram of output voltage V_P, continus V_{out} voltage and primary current

compared to physical reality, parasitic capacitors in parallel of the MOSFETs was used to modelized the imperfection of the transistor. In this case, the voltage difference across the control plates is greater.

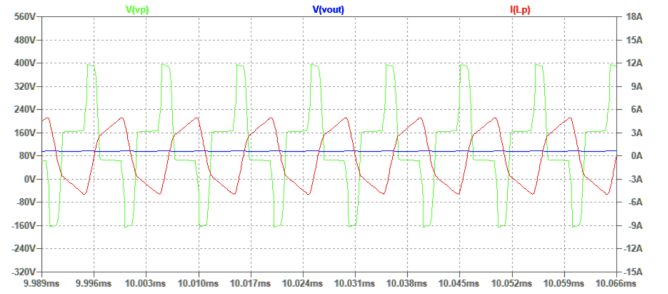

Fig. 6. Chronogram of output voltage V_P, continus V_{out} voltage and primary current

2) MATLAB/Simulink, electrical simulation: As part of this study, a MATLAB/Simulink simulation has been developed in order to validate the DAB. The main goal of this was to compare the converter behaviour obtained from the linearized state space model with the full electric model implemented in Simulink. This approach allows evaluating the precision and relevance of theoretical equations, especially in terms of

dynamics and response at steady state. It is a more representative model of physical reality, integrating non-linearities and losses. We tried to compare the two models through

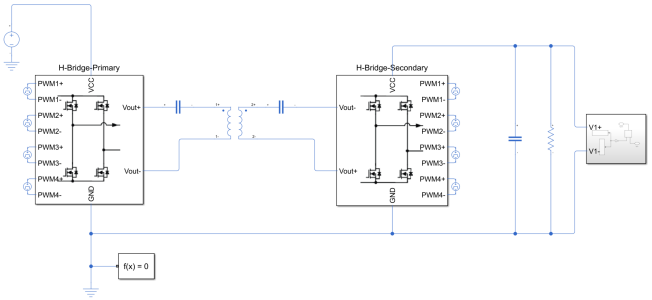

Fig. 7. Global schematic of the DAB into Simulink

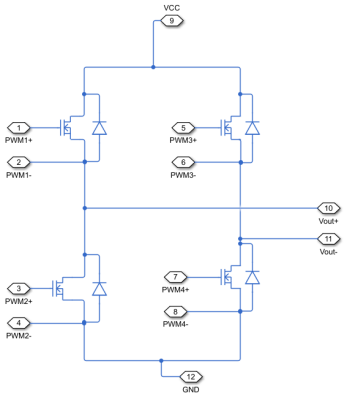

Fig. 8. Inside the H-bridge box

several simulations by varying the working conditions (supply voltage, frequency, duty cycle...), with the aim of identifying possible gap and validate the mathematical model. The LT-

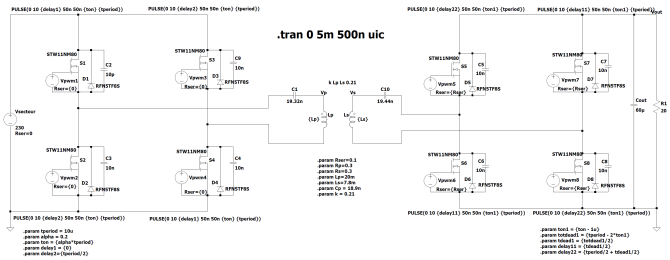

Fig. 9. Global schematics of the DAB into LTSpice

Spice simulation was used as a reference point for the analysis of the converter behaviour. The two models, LTSpice and Simulink, were configured with the same component values (capacitances, inductances, parasitic resistors, etc.), as well as an identical control of the switches (MOSFET transistors). However, despite this consistency in terms of hardware parameters and control strategy, the behaviour observed in the two environments differs significantly, especially regarding energy transfer between the primary and secondary.

In the Simulink model, the logical switch control works correctly, the control signals are applied according to the sequences planned for a DAB, but the current is not transmitted as expected to the secondary, contrary to what is observed in the LTSpice simulation. This divergence remains unexplained at this stage of the study, and several tracks are considered, such as possible differences in component models, taking into account losses or the treatment of magnetic coupling in each of the software. An additional difficulty is that, given the complexity of the wireless resonant energy transfer principle, we do not have a clear reference for the expected waveforms of the output currents and voltages. This lack of reference data makes it difficult to qualitatively analyze the simulation results and validate system behavior in Simulink.

Thus, although the control seems functional and the state space model offers an interesting basis for analysis, the difference in behavior observed between LTSpice and Simulink, despite the use of the same parameters, remains a critical point of our work, requiring further investigation.

3) State space, automatic simulation: Measurement and Characterization of Mutual Inductance in a Coupled Coil System.

E. Measurement and characterisation of mutual inductance an inductive coupling system

1) Reminder on series resonance: Resonance occurs when the coil and capacitor cancel each other out. It is at this point that the total impedance is the smallest, the lowest. The resonant frequency can be expressed as

$$\frac{1}{2\pi\sqrt{LC}}$$

Where L is the coil inductance (in Henry) and C is the capacitor capacitance (in Farad). Figure XX shows a basic circuit used to visualise the resonance phenomenon, which illustrates the typical frequency response showing a resonance peak. In Figure XX, the measured resonance frequency is $f_{resonant} = 159Hz$.

2) Energy transfer system in near field: The mutual inductance M was determined using different methods, where the effect of coil misalignment was also observed.

- Measurement of M using an oscilloscope

A sinusoidal signal was generated using a low-frequency generator with a frequency of 100 kHz. This signal is applied to the primary side of the transmitting coil, so that the mutual inductance M can be calculated from the circuit represented in figure XX.

By using as a hypothesis $r_1 << L_1$, we can write M as

$$M = \frac{|U_2|}{|U_1|} \times L_1$$

where U_1 is the input voltage V, U_2 is the output voltage V and L_1 the self-inductance H. From the input and output volt-

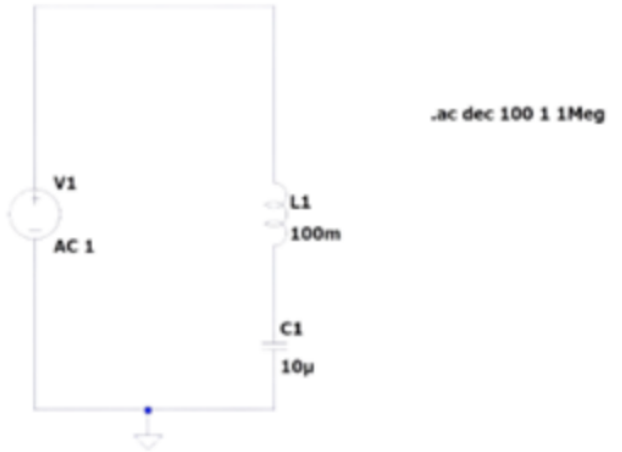

Fig. 10. Electronic circuit LC

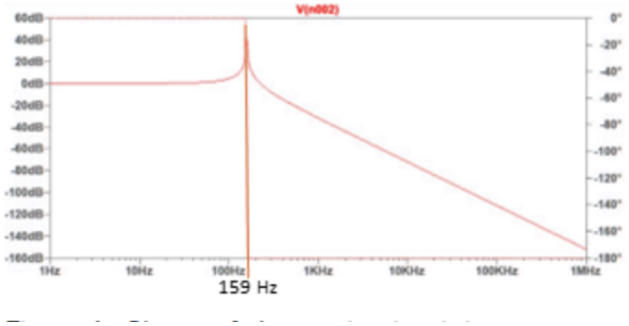

Fig. 11. Shape of electronic circuit in resonance

ages value measured, with the oscilloscope we can calculate the self-inductance such as

$$M = \frac{|0.117|}{|0.362|} \times 28.3 \times 10^{-6}$$

- Measurement of M using a Vectorial Network Analyzer (VNA)

We also used the VNA because, it allowed us to measure the parameters of the scattering parameters in order to deduce the mutual inductance, and visualise the shape of these parameters

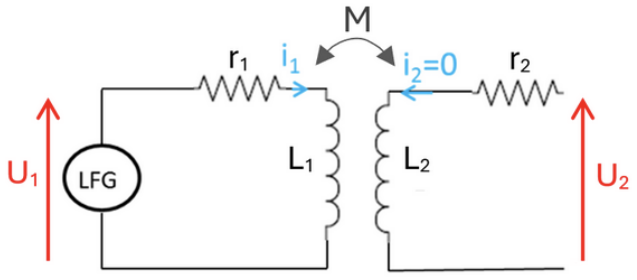

Fig. 12. Schematic of inductive coupling between two coils

in software, so that the resonance peak can be measured accurately and directly measure the system's self-inductance. The figure XX shows the primary, secondary inductance and other data such as the quality factor in the VNA software. Using the VNA, it is possible to characterize a quadripole

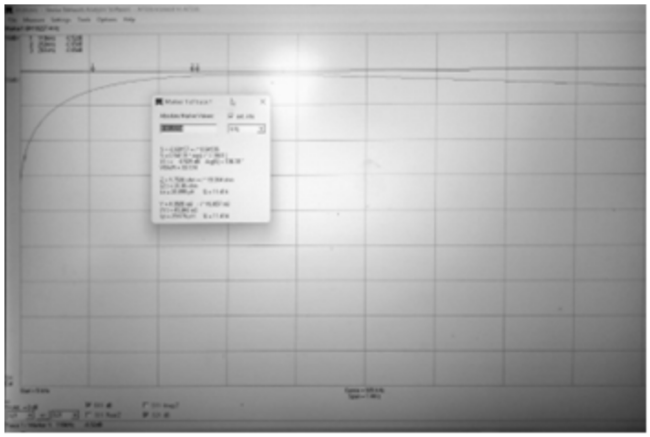

Fig. 13. Software interface for measuring the scattering parameters

(Figure XX). Based on the scattering parameters (also called S-parameters) : $S_{11}, S_{12}, S_{21}, S_{22}$, the value of the mutual inductance can be determined.

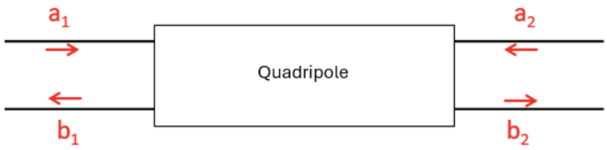

Fig. 14. Software interface for measuring the scattering parameters

$S_{11} = \frac{b_1}{a_1}$ is the input port a_1 reflection coefficient.

$S_{12} = \frac{b_1}{a_2}$ is the reverse gain. It represents to the fraction of the signal transmitted from port 2 to port 1.

$S_{21} = \frac{b_2}{a_1}$ is the forward gain. It represents to the fraction of the signal transmitted from port 1 to port 2.

$S_{22} = \frac{b_2}{a_2}$ is the output port b_2 reflection coefficient

These parameters are used to calculate the mutual inductance M. The measured values obtained are

$$S_{11} = -0.4084794 + i \times 0.3885981$$

$$S_{12} = -0.0878653 + i \times 0.1240676$$

$$S_{21} = -0.0874657 + i \times 0.1235057$$

$$S_{22} = +0.7230404 + i \times 0.6052605$$

In order to compute M :

- Scattering parameters must be converted to Z parameters, the matrix of impedance.
- Take the imaginary part of Z_{21}
- Compute M : $\frac{Im(Z_{21}}{2\pi \times f})$

At the end of the calculations, the value obtained for M is :

$$|M| = 10.930 \times 10^{-6} H$$

The value of L_1 and L_2 were also determined via the interface
$L_1 = 29.076 \times 10^{-6} H$
$L_2 = 28.855 \times 10^{-6} H$

F. Authors and Affiliations

ACKNOWLEDGMENT

The preferred spelling of the word "acknowledgment" in America is without an "e" after the "g". Avoid the stilted expression "one of us (R. B. G.) thanks ...". Instead, try "R. B. G. thanks...". Put sponsor acknowledgments in the unnumbered footnote on the first page.

REFERENCES

Please number citations consecutively within brackets [1]. The sentence punctuation follows the bracket [2]. Refer simply to the reference number, as in [3]—do not use "Ref. [3]" or "reference [3]" except at the beginning of a sentence: "Reference [3] was the first ..."

Number footnotes separately in superscripts. Place the actual footnote at the bottom of the column in which it was cited. Do not put footnotes in the abstract or reference list. Use letters for table footnotes.

Unless there are six authors or more give all authors' names; do not use "et al.". Papers that have not been published, even if they have been submitted for publication, should be cited as "unpublished" [4]. Papers that have been accepted for publication should be cited as "in press" [5]. Capitalize only the first word in a paper title, except for proper nouns and element symbols.

For papers published in translation journals, please give the English citation first, followed by the original foreign-language citation [6].

REFERENCES

[1] G. Eason, B. Noble, and I. N. Sneddon, "On certain integrals of Lipschitz-Hankel type involving products of Bessel functions," Phil. Trans. Roy. Soc. London, vol. A247, pp. 529–551, April 1955.
[2] J. Clerk Maxwell, A Treatise on Electricity and Magnetism, 3rd ed., vol. 2. Oxford: Clarendon, 1892, pp.68–73.
[3] I. S. Jacobs and C. P. Bean, "Fine particles, thin films and exchange anisotropy," in Magnetism, vol. III, G. T. Rado and H. Suhl, Eds. New York: Academic, 1963, pp. 271–350.
[4] K. Elissa, "Title of paper if known," unpublished.
[5] R. Nicole, "Title of paper with only first word capitalized," J. Name Stand. Abbrev., in press.
[6] Y. Yorozu, M. Hirano, K. Oka, and Y. Tagawa, "Electron spectroscopy studies on magneto-optical media and plastic substrate interface," IEEE Transl. J. Magn. Japan, vol. 2, pp. 740–741, August 1987 [Digests 9th Annual Conf. Magnetics Japan, p. 301, 1982].
[7] M. Young, The Technical Writer's Handbook. Mill Valley, CA: University Science, 1989.